Direct Observation of Interphase Composition in Block Copolymers

Kay Saalwächter*

Martin-Luther-Universität Halle-Wittenberg, Institut für Physik, Betty-Heimann-Str. 7, D-06120 Halle, Germany

Yi Thomann and Alfred Hasenhindl

Albert-Ludwigs-Universität Freiburg, Institut für Makromolekulare Chemie und Freiburger Materialforschungszentrum, Stefan-Meier-Str. 21, D-79104 Freiburg, Germany

Horst Schneider

Martin-Luther-Universität Halle-Wittenberg, Institut für Physik, Betty-Heimann-Str. 7, D-06120 Halle, Germany

Received September 15, 2008; Revised Manuscript Received October 8, 2008

ABSTRACT: We demonstrate the fast, direct, and quantitative observation of temperature- and comonomer-induced changes in the interfacial size and composition in phase-separated styrene-butadiene-styrene block copolymers by double-quantum-filtered proton spin-diffusion NMR experiments performed under high-resolution magic-angle spinning conditions. The experiment is based on the dipolar-mediated diffusion of spin magnetization from the (styrenic) rigid phase through a more mobile interphase of variable size and composition into the soft (polybutadiene) domain. The experiment spectroscopically distinguishes between mobilized styrene segments located in the interphase and those mixed (dissolved) in the bulk of the mobile domain. The results indicate that temperature-induced softening due to mobilization of styrene units at the interface and the tendency to become part of an extended interphase is stronger for systems with a lower segregation strength, having statistically distributed styrene comonomers in the soft domain.

Introduction

The understanding of the microphase separation in block copolymers is of central interest for the development and improvement of materials that combine unique thermal and mechanical properties that cannot be realized with single-component systems. Central driving forces for the formation of unique, continuous/dispersed or even cocontinuous structures are the composition, both within and between the different blocks, molecular weight, architecture, and temperature. In the last decades, the importance of the interfacial region (also termed interphase) between the chemically homogeneous (or homogeneously mixed) blocks has received particular attention,[1,2] as it affects the thermal and mechanical properties of the material. A variety of experimental techniques, such as electron microscopy,[3] small-angle X-ray scattering,[4] neutron scattering and reflectivity,[5,6] and deuterium NMR[7−9] was used to study compositional, density, or mobility profiles across the interface. The mentioned methods are, however, indirect, as they are only sensitive to electron density changes, or require interface-specific isotope labeling, respectively.

As an alternative, proton spin diffusion NMR, exploiting for instance mobility differences between hard (below T_g) and soft (above T_g) regions, has long been recognized to be sensitive to the size of the microphases as well as an interphase.[10−13] In such experiments, the initial proton magnetization is selectively suppressed in one of the phases (most often the rigid phase, using "dipolar filters" that suppress signal from strongly dipolar-coupled segments), and then re-equilibrates due to an also dipolar-mediated flip-flop process that has the characteristic of a diffusion process and provides spatial information.

Generally, interfacial mobility differences are rather easy to quantify by NMR even under low-resolution conditions, simply by suitable signal decomposition.[14] However, true *composition* gradients inevitably require chemical resolution, that is, high-resolution spectra. This was demonstrated many times, mainly by ^{13}C-detected spin diffusion experiments based on a combination of a suitable magnetization filter and spin diffusion on the ^{1}H channel with cross-polarization magic-angle spinning (CP/MAS) detection.[10,11,13] Disadvantages of these powerful techniques are, however, the increased experimental time due to low ^{13}C sensitivity and the inherently nonquantitative CP transfer.

Proton-only NMR, on the other hand, solves these problems, as the full sample polarization is always under experimental control.[15] Given sufficient mobility and sufficiently resolved ^{1}H spectral lines, moderate MAS (on the order of 5 kHz) is in fact a suitable and simple method for the chemically resolved study of the composition of soft and interfacial polymer domains that are well above the glass transition. As an example, ^{1}H MAS in combination with mobility-based signal suppression of rigid and interfacial components by dipolar filter variation and spin diffusion has recently been used for the study of the interfacial size in PEO-PPO triblock copolymers.[16] Herein, we demonstrate for the first time that the combination of a more recently introduced double-quantum (DQ) filter that selects the rigid-phase magnetization[17,18] with chemically specific detection under moderate MAS is probably the most direct and efficient experiment to elucidate the size and the composition of the interphase in typical hard−soft systems, that is, styrene-butadiene-styrene (SBS) copolymers. The experiment exploits the diffusive progress of magnetization from the rigid phase, which in SBS is predominantly composed of polystyrene (PS),[19,20] first through the compositional (yet sufficiently mobile) interphase into the bulk mobile phase that is mostly polybutadiene (PB). In a series of preliminary experiments, we demonstrate the dependence of the interfacial size and composition on temperature and the segregation strength, varied by introducing styrene comonomers in the soft phase.

* To whom correspondence should be addressed. E-mail: kay.saalwaechter@physik.uni-halle.de.

10.1021/ma802094h CCC: $40.75
Published on Web 11/06/2008

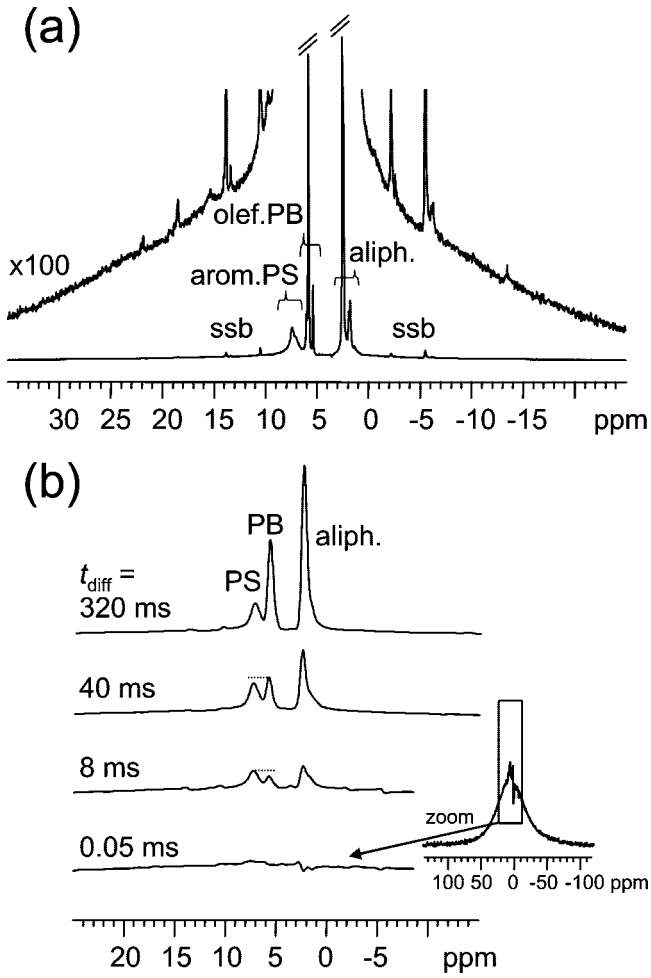

Figure 1. (a) ^{1}H MAS spectrum and magnification showing the broad rigid (PS) background (ssb: spinning sidebands) and (b) DQ-filtered spectra after different spin diffusion times. Additional Gaussian line broadening was applied for the latter to reduce subtraction artifacts from the DQ filter, resulting in single peaks for aromatic (PS), olefinic (PB) and aliphatic resonance groups. The broad PS hump is hardly visible on the shown spectral scale, as is obvious from the inset showing the full 0.05 ms spectrum.

Experimental Section and Theory

Samples. Two commercial SBS triblock structures have been studied, first, an asymmetric star with PB at the core and three short and one long PS arm, with size ratio 1:9 (K-Resin KR03, Chevron Phillips), and an equivalent structure with a statistical poly(styrene-*co*-butadiene) core containing about 15%w/w PS (Styrolux 3G55, BASF). Both polymers have the same PB content of about 25%w/w. The approximate molecular weights M_n (GPC, PS standard) are 99 and 86 kg/mol, respectively, both with polydispersity PD $\approx$ 2.1. As addressed in a more detailed study using low-field ^{1}H NMR and TEM,[19,20] the polymers form disordered lamellar microdomains with a soft-phase thickness of about 13–14 nm at room temperature.

NMR spectroscopy. ^{1}H NMR experiments were performed on a Bruker Avance 500 spectrometer (B_0 = 11.7 T), using a Bruker 4 mm MAS double-resonance probe at 4 kHz spinning frequency and 90° pulses of about 3.2 μs length. The spectral width was 320 ppm (160 kHz) to cover the broad rigid-phase (PS) signal. The baseline was offset-corrected before integration of the full (rigid + mobile) sample signal. For separate integration of the individual resolved mobile- and interphase signals, a narrow 30 ppm region around the sharp signals was baseline-corrected using a second-order polynomial, thus removing the PS background hump. This is easily possible, as is obvious from the comparison of the lower spectrum in Figure 1b and the inset. The integrations yield the overall mobile fraction, f_{mob}, and the fraction of PS in the mobile phase, f'_{PSmob}. Note that the latter refers to the mobile phase (=100%) as reference; the corresponding overall signal fraction is $f_{mob} \times f'_{PSmob}$. It is obtained by correcting the intensity of the aromatic (PS) and olefinic (PB) resonances with respect to the overall monomer proton contents (see Figure 1a). A minor rigid-phase signal loss of less than 10% during the 4.5 μs dead time was not corrected in this study and leads to small systematic errors in the phase compositions and domain sizes.

Table 1. Signal Fractions from Spectrum Integration, Results from Initial-Slope Analyses, and Interphase Parameters for the Simulated Curves in Figure 2[a]

sample	temp (K)	f_{mob} (%)	f'_{PSmob} (%)	t_0 (ms)	d_{rig} (nm)	d_{mob}[b] (nm)	a (%)	s (%)	$f'_{PSmob}(\infty)$ (%)
K-Resin	309	33	4.8	2260	42	17	12	25	3
	363	40	17.5	2160	38	21	21	90	3
Styrolux	309	40	18.5	1005	28	15	10	50	18
	363	53	34.5	670	21	20	97	27	18

[a] Calculated from d_{rig}, f_{mob}, and the spin densities assuming lamellar arrangement. [b] For the simulations, only a and s were varied, while $f'_{PSmob}(\infty)$ results from eq 2.

The DQ-filtered spin diffusion pulse sequence is identicial to a conventional DQ build-up experiment with variable z-filter, and reads 90_x-τ_{DQ}-90_{-x}-2 μs-$90_{\phi1}$-τ_{DQ}-$90_{-\phi1}$-t_{diff}-$90_{\phi2}$-$acq_{\phi3}$. The phase cycle involves CYCLOPS on the read-out pulse ($\phi2$) and a four-step DQ filtration cycle on the second (reconversion) pulse pair ($\phi1$) and the receiver ($\phi3$):

$$\varphi1 = \{x, y, -x, -y\}$$
$$\varphi2 = \{4\times(x),\ 4\times(y),\ 4\times(-x),\ 4\times(-y)\}$$
$$\varphi3 = \{x, -x, x, -x, y, -y, y, -y, -x, x, -x, x, -y, y, -y, y\}$$

A phase-cycle controlled 90_x-2 μs-90_y-2 μs-$90_{\pm x}$ composite magnetization inversion was applied prior to the sequence for alternate storage along $+z$ and $-z$ for the first and second block of 16 transients, respectively, thus avoiding potential T_1-related artifacts.[20] The receiver phase $\phi3$ is inverted accordingly for the second half. The inversion was also used in front of simple one-pulse MAS spectra acquisitions to suppress potential probe background. A DQ excitation and reconversion time τ_{DQ} of 15 μs was used for maximum hard-phase signal retention, with negligible inter- and mobile-phase magnetization. For such a short DQ time and moderate MAS frequencies, a rotor synchronization is not possible, which leads to an overall DQ conversion of about 25% as opposed to a theoretical maximum on the order of 50%, which is in fact realized under static conditions.[20] The lower efficiency, combined with secondary effects such as coil vibrations, leads to some spurious correlated noise in the spectra (see inset in Figure 1b). For the present study, this noise was the major limiting factor for the accuracy of the method, as it affects the accurate determination of intensities at very short spin diffusion times. More appropriate dedicated rotor-synchronized DQ recoupling sequences will be tested in the future.

Analysis of Spin Diffusion Data. The full relative source (rigid) and sink (interface and mobile) phase signals, normalized and corrected for T_1 relaxation effects at long times by division through the full (rigid + mobile) signal, were plotted vs $\sqrt{t_{diff}}$, and domain sizes were obtained from the common initial-slope approach,[20−22] using temperature-dependent spin diffusion coefficients obtained from T_2 measurements at low field.[20,22] The results are collected in Table 1. Note that the initial-slope approach yields the size of the source domain, that is, a DQ-filtered, rigid-phase-selected experiment yields the rigid domain size. The influence of 4 kHz MAS on the spin diffusion coefficients was not taken into account. According to a very recent study,[23] a reduction on the order of 30% can be expected for both rigid and mobile phases, thus explaining that the results for the domain sizes of K-Resin are about 20% larger than reported in our earlier paper.[20]

Spin diffusion curves corresponding to the overall $f_{mob}(t_{diff})$ and the composition-resolved $f_{mob}(t_{diff}) \times f'_{PSmob}(t_{diff})$ were simulated using a modified home-written program presented in our earlier

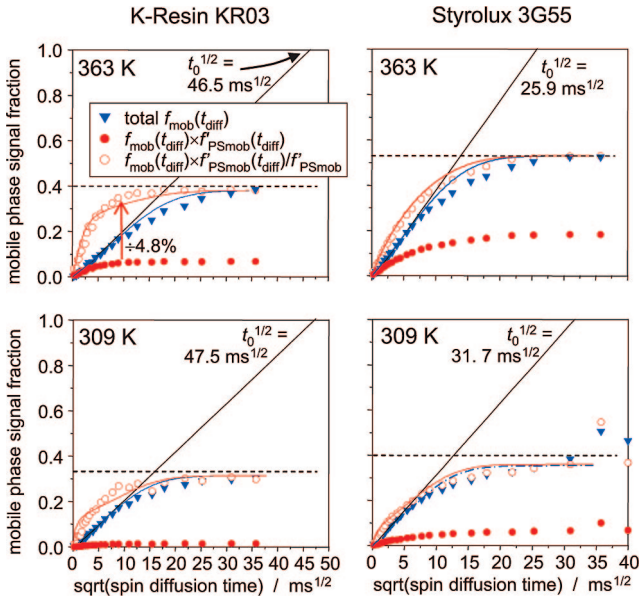

Figure 2. Double-quantum spin diffusion data for the two samples at two different temperatures. Solid lines are from simulations with parameters given in Table 1, straight lines are from the initial-slope analysis, and dashed lines indicate the mobile fraction ($1 - f_{rig}$) from the spectrum integrations.

work,[20] where all important parameters are compiled. The simulations start with an initially polarized rigid region, and the signal fractions in the interphase and mobile regions are extracted on the basis of the advancing magnetization profile in combination with a given composition profile.

Essential parameters are the spin diffusion coefficients, spin densities, domain sizes, and, for the main purpose of this work, the composition profile $\phi_{PS}(x)$, whose origin is located at the center of the rigid domain. The spin diffusion coefficient of the interphase was taken as identical as for the mobile phase, which is supported by our finding that the mobile-phase T_2 relaxation was nearly monoexponential in all cases.[19] Note that the composition profile has a larger spatial extent than the rather narrow mobility gradient region identified in our earlier work.[20] The local spin densities in the interphase and the bulk of the mobile domain were calculated according to $\phi_{PS}(x)$ by interpolation between ρ_{PS} and ρ_{PB}. Effects of different phase-specific T_1 relaxation times,[20] which are important at lower field (where T_1 is often shorter) and at longer spin diffusion times, were not taken into account.

The rigid (d_{rig}) and interphase + mobile (d_{mob}) thicknesses were held constant at the values obtained from initial-slope analysis (and confirmed by two-phase fits), leaving a single free size parameter a describing the interphase width as a fraction of the overall mobile phase, $2d_{if} = a \times d_{mob}$ (a mobile layer is flanked by two interphases). To keep the number of parameters at a minimum, the composition profile (see Figure 3a) is described by only two more parameters: a finite and constant PS fraction for the bulk of the mobile phase, $f'_{PSmob}(\infty)$, describing PS comonomers and completely dissolved PS subchains, and a shape parameter s ranging from 0 to 1 describing different composition profiles in the interphase. The profile is modeled according to

$$\varphi_{PS}(x) = [1 - f'_{PSmob}(\infty)]\left[1 - \left(\frac{x - d_{rig}/2}{d_{if}}\right)^{\frac{s}{(1-s)}}\right] + f'_{PSmob}(\infty) \quad (1)$$

in the interphase region between $d_{rig}/2 \le x \le (d_{rig} + ad_{mob})/2$, and values of 1 and $f'_{PSmob}(\infty)$ below and above, respectively. The periodic lamellar morphology is obtained by taking $x = 0$ and $x = d_{rig}/2 + d_{mob}/2$ as mirror planes. The interphase term was chosen on a purely heuristic basis, as it gives a linear decay (constant gradient) for $s = 0.5$, concave shapes for smaller s, and convex shapes for larger s. Conveniently, s is exactly the area fraction under the function in square brackets (when x is taken as dimensionless). Importantly, the three parameters are interdependent, as they must be chosen such that the complete mobile PS fraction, which is directly measurable and given by the integral of $\phi_{PS}(x)$ over the full mobile phase, is constant

$$f'_{PSmob} = f'_{PSmob}(\infty) + s\,a(1 - f'_{PSmob}(\infty)) \quad (2)$$

In this model, the rigid phase is assumed to consist of PS only, in agreement with previous findings[19,20] and phase-specific ^{13}C spectra based on a very short CP (not shown).

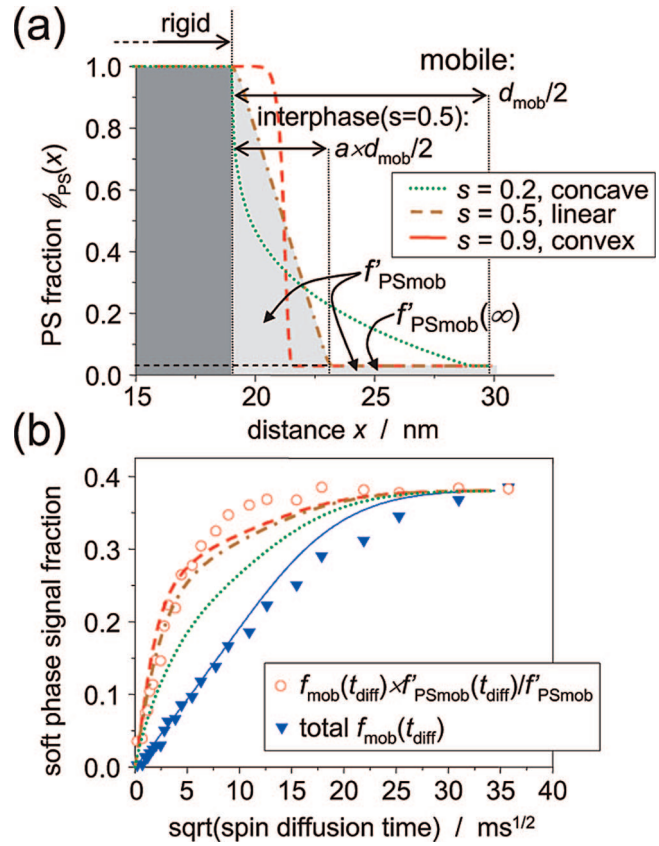

Figure 3. (a) Different PS proton fraction profiles compatible with an 18% overall mobile-phase PS fraction for K-Resin KR03 at 363 K, and (b) experimental data along with corresponding simulation results. The solid line is a simulation of the total mobile fraction in a two-component scenario (rigid and mobile), using fixed parameters from the initial-slope analysis. The other lines correspond to simulations of the PS-detected signal fraction (open circles), based on the concentration profiles in (a).

Results and Discussion

A typical 4 kHz-MAS ^1H spectrum of an SBS block copolymer is shown in Figure 1a. Aromatic, olefinic, and aliphatic sites are readily resolved, and the unresolved rigid-phase signal forms a broad hump. The power of the DQ-filtered spin diffusion experiment is readily apparent from Figure 1b, where the aromatic PS resonances obviously rise more quickly (the signal being even higher than the olefinic PB signal at 8 ms spin diffusion time). This immediately proves that the magnetization first diffuses through a PS-rich, yet mobile interphase. At long spin diffusion times, the ratio between the two resonances reaches the ratio f'_{PSmob} that is calculated from the integration of the ^1H MAS spectrum.

For a more quantitative evaluation, signal fractions for the overall mobile phase and its PS fraction are plotted in Figure

2 for the two different samples and different temperatures. The effect of the quicker rise of the mobile PS signal is most readily appreciated if the mobile PS fraction, $f_{mob}(t_{diff}) \times f'_{PSmob}(t_{diff})$, is divided by the overall f'_{PSmob} (open circles). These curves then reach the same plateau as the overall mobile fraction, $f_{mob}(t_{diff})$, but they rise more quickly when PS is accumulated in the interphase. Our simulations showed that for certain values for the domain sizes, these curves can even exhibit maxima, indicating very sharp $\phi_{PS}(x)$. Another diagnostic and very interesting case is represented by the data for Styrolux 3G55 at low temperature (lower right), where the PS-specific data almost parallels the overall $f_{mob}(t_{diff})$. This proves directly that the PS is in this system almost uniformly distributed over the whole mobile domain at low temperature, and that the PS that is mobilized upon heating (at the mobility interface) spreads quite much into the bulk of the mobile domain, since the difference between the two curves is bigger, but still not very high at 363 K. To the contrary, the softened PS in K-Resin remains closer to the interface, as is directly seen in the corresponding data.

More quantitatively, the data was simulated according to the procedures outlined above. The simulated curves are also shown in Figure 2, and the simulation parameters are collected in Table 1 (only the three in the last columns were varied). As the three parameters, the PS fraction in the bulk of the mobile phase f'_{PSmob} (∞), the interphase size fraction a, and the shape parameter s are interdependent and related to the overall PS content of the mobile phase, we have effectively varied only s and a. Further ambiguities are lifted by combining experiments at different temperature. At low temperature, the interphase is small ($a \approx 10\%$), and the approximate f'_{PSmob} (∞) was estimated to 3% for K-Resin KR03 and 17% for Styrolux 3G55, in accordance with the sample properties. These values were held constant for the high-temperature case, leaving a single free parameter that was fitted by eye.

The central results of this preliminary report are apparent from the simulation parameters in Table 1. In K-Resin, the mobile PS fraction increases from 5 to 18%, and the simulations clearly show that this PS is confined to rather narrow interphases ($a \approx$ 20%, i.e., 2×2 nm). In contrast for Styrolux, while the amount of mobilized PS is somewhat larger but similar in magnitude, it extends much more into the mobile phase (2×9.5 nm interphase with concave ϕ_{PS} and only 1 nm unchanged core mobile phase). This can directly be attributed to the decreased segregation strength of a statistical PB/PS block versus a homo-PB block in the latter system.

The second important aspect is that the method is indeed sensitive to the *shape* of the composition profile, which allows theoretical predictions to be put to a more rigorous test. Figure 3a shows different concave, linear constant-gradient, and convex interphase composition profiles compatible with the known overall f'_{PSmob}, and in Figure 3b the corresponding simulations are compared with the data. The convex profile can immediately be excluded, while the best fit is provided by a linear to concave shape. This tendency toward a styrene-rich interface in well segregated copolymers fully support earlier indirect claims of an asymmetric interface composition.[1,3,7] In contrast, the high-temperature data of Styrolux (see Figure 2) can only be fitted with an extended convex profile ($a = 0.97$ and $s = 0.27$, see Table 1), similar to the dotted lines in Figure 3a,b.

At this point, our simulation procedure still needs to be improved for more precise predictions. Notably, the simulations for the total $f_{mob}(t_{diff})$ deviate from the data at t_{diff} beyond 100 ms (10 $ms^{1/2}$), as do the plateaus at lower temperatures. This is attributed to T_1 relaxation effects, which are different for the two phases. With mobile-phase, T_1s on the order of 1.3 to 1.7 s in the temperature interval studied (and rigid-phase T_1s being larger), differential mobile-phase signal losses on the 100 ms time scale cannot be neglected. In fact, in our low-field spin diffusion study of the same material,[20] perfect fits were possible, taking into account differential T_1 relaxation. Clearly, these effects must be accounted for at high field when simulations rather than initial-slope analyses are performed but were beyond the scope of this preliminary report. The data up to $\sqrt{t_{diff}}$ is considered reliable because the overall signal loss is less than 10%.

We finally summarize that the technique, within the confines of ambiguities set by the analysis of the advancing diffuse magnetization profile, provides fully quantitative information on the chemical composition profile in the soft phase of any block copolymer structure with sufficient mobility contrast. A study of composition profiles in the hard phase (with the mobile domain as starting phase using a different dipolar filter) could also be envisioned, yet it would inevitably be less direct. One could either retain the quantitative aspect by observing protons and using very fast MAS ($\geq$30 kHz) and high fields ($\geq$600 MHz), requiring the resolution of ambiguities in phase-specific detection (by deconvolution of lines with different width) and severely reduced spin diffusion coefficients.[23] An alternative is of course the well established, but more time-consuming and less quantitative indirect observation via a short, thus rigid-phase specific cross-polarization to ^{13}C.[10,11,13]

A possible limitation that has as yet not been addressed in the spin diffusion literature is the distinction between a faster intrachain transfer (along a curvilinear path) and a slower, interchain transfer, in particular for the mobile phase. This would correspond to locally anisotropic spin diffusion effects as a result of different intra- and interchain residual dipolar couplings. Such effects would challenge the direct relation between spin diffusion time and spatial extent of the magnetization profile, and could lead to systematic errors in the composition profiles. We feel that these effects are not too important, as they could not account for the difference between the K-Resin and Styrolux samples, but further work to elucidate such effects appears highly worthwhile.

Conclusions

We have shown that the DQ-filtered proton MAS spin diffusion technique is very suitable to directly detect changes in the interfacial size and composition in the mobile domain of different SBS block copolymers at different temperatures. The results indicate that temperature-induced softening due to mobilization of styrene units at the interface and their tendency to become part of an extended interphase is stronger for systems with lower segregation strength, having statistically distributed styrene comonomers in the soft domain. The technique will be of use for more systematic studies in similar block copolymers systems with sufficient T_g contrast. We are currently pursuing applications to more well-defined monomodal systems and mixtures to more systematically address the influence of segregation strength and polydispersity on size and composition of the interphase. An improved and more efficient version of the experiment will employ a dedicated MAS DQ recoupling sequence that can be incremented in small time steps to realize short DQ excitation times, and the data analysis will be improved by taking T_1 effects into account and testing least-squares fitting approaches as well as data inversion strategies that may directly yield the interphase composition profile.

Acknowledgment. Funding of this work was provided by the Deutsche Forschungsgemeinschaft (SFB 418) and the Fonds der Chemischen Industrie.

References and Notes

(1) Henderson, C. P.; Williams, M. C. Asymmetric composition profiles in block copolymer interphases: 1. Experimental evidence. *Polymer* **1985**, *26*, 2021–2025.

(2) Henderson, C. P.; Williams, M. C. Asymmetric composition profiles in block copolymer interphases: 2. Thermodynamic model predictions and implications. *Polymer* **1985**, *26*, 2026–2038.

(3) Spontak, R. J.; Williams, M. C.; Agard, D. A. Interphase composition profile in SB/SBS block copolymers, measured with electron microscopy, and microstructural implications. *Macromolecules* **1988**, *21*, 1377–1387.

(4) Hashimoto, T.; Shibayama, M.; Kawai, H. Domain-boundary structure of styrene-isoprene block copolymer films cast from solution. 4. Molecular-weight dependence of lamellar microdomains. *Macromolecules* **1980**, *13*, 1237–1247.

(5) Anastasiadis, S. H.; Russell, T. P.; Satija, S. K.; Majkrzak, C. F. The morphology of symmetric diblock copolymers as revealed by neutron reflectivity. *J. Chem. Phys.* **1990**, *92*, 5677–5691.

(6) Noro, A.; Okuda, M.; Odamaki, F.; Kawaguchi, D.; Torikai, N.; Takano, A.; Matsushita, Y. Chain localization and interfacial thickness in microphase-separated structures of block copolymers with variable composition distributions. *Macromolecules* **2006**, *39*, 7654–7661.

(7) Stöppelmann, G.; Gronski, W.; Blume, A. Motional heterogeneity and the nature of the interphase in block copolymers: A ^{2}H nuclear magnetic resonance study. *Polymer* **1990**, *31*, 1838–1853.

(8) Mukai, U.; Gleason, K. K.; Argon, A. S.; Cohen, R. E. Poly(dimethylsiloxane)/nylon-6 block copolymers: Molecular mobility at the interface. *Macromolecules* **1995**, *28*, 4899–4903.

(9) Zumbulyadis, N.; Landry, M. R.; Russell, T. P. Interphase mixing in symmetric diblock copolymers determined by proton−deuterium CP/MAS NMR. *Macromolecules* **1996**, *29*, 2201–2204.

(10) Clauss, J.; Schmidt-Rohr, K.; Spiess, H. W. Determination of domain sizes in heterogeneous polymers by solid-state NMR. *Acta Polym.* **1993**, *44*, 1–17.

(11) Cai, W. Z.; Schmidt-Rohr, K.; Egger, N.; Gerharz, B.; Spiess, H. W. A solid-state NMR study of microphase structure and segmental dynamics of poly(styrene-*b*-methylphenylsiloxane) diblock copolymers. *Polymer* **1993**, *34*, 267–276.

(12) Landfester, K.; Spiess, H. W. Characterization of interphases in core−shell latexes by solid-state NMR. *Acta Polym.* **1998**, *49*, 451–464.

(13) Jack, K. S.; Wang, J.; Natansohn, A.; Register, R. A. Characterization of the microdomain structure in polystyrene−polyisoprene block copolymers by ^{1}H spin diffusion and small-angle X-ray scattering methods. *Macromolecules* **1998**, *31*, 3282–3291.

(14) Tanaka, H.; Nishi, T. Study of block copolymer interface by pulsed NMR. *J. Chem. Phys.* **1985**, *82*, 4326–4331.

(15) Maus, A.; Hertlein, C.; Saalwächter, K. A robust proton NMR method to investigate hard/soft ratios, crystallinity, and component mobility in polymers. *Macromol. Chem. Phys.* **2006**, *207*, 1150–1158.

(16) Sun, P.; Dang, Q.; Li, B.; Chen, T.; Wang, Y.; Lin, H.; Jin, Q.; Ding, D. Mobility, miscibility, and microdomain structure in nanostructured thermoset blends of epoxy resin and amphiphilic poly(ethylene oxide)-*block*-poly(propylene oxide)-*block*-poly(ethylene oxide) triblock copolymers characterized by solid-state NMR. *Macromolecules* **2005**, *38*, 5654–5667.

(17) Ba, Y.; Ripmeester, J. A. Multiple quantum filtering and spin exchange in solid state nuclear magnetic resonance. *J. Chem. Phys.* **1998**, *108*, 8589–8594.

(18) Buda, A.; Demco, D. E.; Bertmer, M.; Blümich, B.; Reining, B.; Keul, H.; Höcker, H. Domain sizes in heterogeneous polymers by spin diffusion using single-quantum and double-quantum dipolar filters. *Solid State Nucl. Magn. Reson.* **2003**, *24*, 39–67.

(19) Thomann, Y.; Thomann, R.; Saalwächter, K.; Heck, B.; Hasenhindl, A.; Knoll, K.; Steininger, H.; Mülhaupt, R. Gradient interfaces in SBS and SBS/blends and their influence on morphology development and mechanical properties. *Macromolecules* **2008**, submitted for publication.

(20) Mauri, M.; Thomann, Y.; Schneider, H.; Saalwächter, K. Spin diffusion NMR at low field for the study of multiphase solids. *Solid State Nucl. Magn. Reson.* **2008**, *34*, 125–141.

(21) Schmidt-Rohr, K.; Spiess, H. W. *Multidimensional Solid-State NMR and Polymers*; Academic Press: London, 1994.

(22) Mellinger, F.; Wilhelm, M.; Spiess, H. W. Calibration of ^{1}H NMR spin diffusion coefficients for mobile polymers through transverse relaxation measurements. *Macromolecules* **1999**, *32*, 4686–4691.

(23) Jia, Z.; Zhang, L.; Chen, Q.; Hansen, E. W. Proton spin diffusion in polyethylene as a function of magic-angle spinning rate. A phenomenological approach. *J. Phys. Chem. A* **2008**, *112*, 1228–1233.

MA802094H